9-1-1997

X-ray-Absorption Spectral Study of the $R_2Fe_{17-x}M_x$ Solid Solutions (R=Ce, Nd and M=Al, Si)

Denis Vandormael

Fernande Grandjean
Missouri University of Science and Technology, grandjeanf@mst.edu

Valérie Briois

D. P. Middleton

et. al. For a complete list of authors, see http://scholarsmine.mst.edu/chem_facwork/832

Recommended Citation

D. Vandormael et al., "X-ray-Absorption Spectral Study of the $R_2Fe_{17-x}M_x$ Solid Solutions (R=Ce, Nd and M=Al, Si)," *Physical Review B (Condensed Matter)*, vol. 56, no. 10, pp. 6100-6106, American Physical Society (APS), Sep 1997.
The definitive version is available at https://doi.org/10.1103/PhysRevB.56.6100

X-ray-absorption spectral study of the $R_2Fe_{17-x}M_x$ solid solutions (R=Ce, Nd and M=Al, Si)

D. Vandormael and F. Grandjean
Institute of Physics, B5, University of Liège, B-4000 Sart-Tilman, Belgium

V. Briois
Laboratoire pour l'Utilisation du Rayonnement Electromagnétique, Bâtiment 209D, Université Paris-Sud, F-91405 Orsay, France

D. P. Middleton
Philips Research Laboratories, NL-5600 JA Eindhoven, the Netherlands

K. H. J. Buschow
Van der Waals-Zeeman Institute, University of Amsterdam, NL-1018 XE Amsterdam, the Netherlands

Gary J. Long
Department of Chemistry, University of Missouri-Rolla, Rolla, Missouri 65409-0010
(Received 14 February 1997; revised manuscript received 5 May 1997)

The x-ray-absorption near-edge structure (XANES) spectra obtained at the cerium L_{III} edge of the $Ce_2Fe_{17-x}Al_x$ solid solutions and $Ce_2Fe_{14}Si_3$ show two absorption peaks characteristic of the $4f^1$ and $4f^0$ configurations of cerium, peaks which indicate that cerium is in a mixed valent state in these compounds. All the XANES spectra have been consistently and excellently fit with one sigmoidal function and two Gaussian-broadened Lorentzian functions. The cerium spectroscopic valence obtained from the relative areas of the two peaks decreases from 3.64 to 3.43 between $x=0$ and 9 in $Ce_2Fe_{17-x}Al_x$, and correlates linearly with the cerium site volume. This correlation confirms that the cerium valence is strongly dependent upon steric effects. In contrast, the cerium valence obtained from the XANES spectrum of $Ce_2Fe_{14}Si_3$ is not determined by steric effects and indicates, in agreement with other measurements and calculations, that silicon is more covalently bonded with its near-neighbor cerium atoms than is aluminum. The neodymium L_{III}-edge XANES spectra of the $Nd_2Fe_{17-x}Al_x$ solid solutions, where x is 0, 3, and 8, reveal the presence of only trivalent neodymium and an increase of the empty $5d$ state density when aluminum is substituted in place of iron. XANES measurements at the iron K edge of the $Ce_2Fe_{17-x}Al_x$ and $Nd_2Fe_{17-x}Al_x$ solid solutions show changes in the relative intensity of the multiple scattering peaks, changes which are related to the changing composition of the first three neighbor shells with increasing aluminum content. [S0163-1829(97)09034-6]

I. INTRODUCTION

The valence state of cerium in intermetallic magnetic compounds has recently attracted[1–6] a renewed interest because of the investigative possibilities provided by synchrotron radiation. Indeed, there is a close connection between the valence and the magnetic character of cerium. In intermetallic compounds with transition metals, cerium is more often found in the nonmagnetic and strongly mixed valent α state, than in the magnetic trivalent γ state. Whereas in the α state, the cerium $4f$ wave function is strongly hybridized[7] with the $(5d6s)^3$ wave function, in the γ state, the $4f$ wave function is almost atomiclike and produces a large magnetic anisotropy. Further, in the γ state the cerium magnetic moment is close to $2.54\mu_B$, the theoretical magnetic moment of trivalent cerium. In the above and subsequent discussion it is very important to note that the terms valence and valence state are not used in the sense of chemical oxidation state and trivalent and mixed valent do not correspond to cerium in the +3 or a higher oxidation state. Indeed cerium in both the α state and γ state is neutral in terms of the charge balance, as expected in the metal.

In the search for permanent magnetic materials, the cerium intermetallic compounds of the Ce_2Fe_{17} and $Ce_2Fe_{14}B$ type are interesting because cerium is an abundant and inexpensive rare-earth element. However, it is important that these cerium based materials contain some γ-like cerium to contribute both to the magnetic anisotropy as well as the total magnetization. There are only a few techniques available to investigate the valence state of cerium in intermetallic compounds. X-ray photoelectron spectroscopy[7] has been used to study $CeRu_2$ and $Ce_2Fe_{14}B$. More recently, the availability of tunable x-ray sources at various synchrotron facilities has provided[1–6] the possibility of determining the cerium valence by x-ray absorption at the cerium L_{III} edge.

A comparison of the cerium valence states reported by different research groups for the same compounds indicates that the actual value of the valence strongly depends on the model used to analyze the data. For example, the values found for Ce_2Fe_{17} vary from 3.58 in Ref. 2 to 3.33 in Refs. 1 and 3, and the values for $Ce_2Fe_{14}B$ vary from 3.44 in Ref. 2 to 3.33 in Ref. 1. Further, as stressed by Capehart *et al.*,[5] the spectroscopic valence, determined from the cerium L_{III}-edge absorption spectrum, should not be taken as the literal chemical valence of cerium. Changes observed in the cerium absorption spectrum reflect changes in the f electron configuration of cerium and the valence deduced from x-ray-absorption near-edge structure (XANES) measurements is simply a way to quantify these changes. Hence, trends in the values are meaningful but, as mentioned above, the actual values do not correspond to the chemical oxidation of cerium, but rather to the transfer of cerium electrons from bound states to conduction bands in the compounds.

Previous studies on the interstitial hydrides[2,3] and nitride[6] of Ce_2Fe_{17} and $Ce_2Fe_{14}B$ have shown that the cerium valence is affected by the insertion of hydrogen or nitrogen into the intermetallic compound, even if this conclusion has lead to some controversy[4,5] in the case of $Ce_2Fe_{14}B$ and its hydride. Furthermore, a steric or volume effect on the cerium valence has been observed both in Ce_2Fe_{17} and its hydrides[3] and in $Ce_2Fe_{14}B$ and its hydride.[2] However, this steric effect has been viewed differently in the two papers. In the $Ce_2Fe_{17}H_x$ series, the cerium valence decreases[3] from 3.33 in Ce_2Fe_{17} to 3.26 in $Ce_2Fe_{17}H_5$ concurrently with an increase in unit cell volume, from 775 to 816 Å^3. In $Ce_2Fe_{14}B$ and $Ce_2Fe_{14}BH_x$, the cerium valence decreases[2] from 3.44 to 3.36, with an increase in cerium site volume from 32.5 to 33.5 Å^3. In the case of $Ce_2Fe_{17}H_5$, the cerium site volume is actually smaller than in Ce_2Fe_{17} because of the presence of the additional interstitial hydrogen near neighbors, even though $Ce_2Fe_{17}H_5$ has a larger unit cell volume than Ce_2Fe_{17}. Hence, the cerium valence in the $Ce_2Fe_{17}H_x$ series, when plotted as a function of the cerium site volume, decreases with decreasing site volume in disagreement with the conclusion of Capehart *et al.*[2,5] Such a contradictory behavior of the unit cell and cerium site volume does not exist with the substituted compounds studied herein. These difficulties show that the interpretation of the words ''valence'' and ''steric effect'' is delicate and difficult.

It is well known that the substitution of iron by other metals may also improve the magnetic properties of Ce_2Fe_{17}. The $Ce_2Fe_{17-x}Al_x$ and $Ce_2Fe_{17-x}Si_x$ solid solutions have been extensively studied[8–11] by magnetic measurements, neutron diffraction, Mössbauer spectroscopy, and electrical resistivity measurements. For our purpose herein, the important conclusions from these studies are that in both series a maximum Curie temperature is observed for x equal to ca. 3 and that in $Ce_2Fe_{17-x}Al_x$ the unit cell volume increases with increasing x, whereas in $Ce_2Fe_{17-x}Si_x$, it decreases with increasing x.

In order to both investigate the effect of the substitution of the iron in Ce_2Fe_{17} by aluminum or silicon on the cerium valence, and to confirm the validity of the steric effect observed by Capehart *et al.*,[2,5] we have carried out XANES measurements at the cerium L_{III} edge in both $Ce_2Fe_{17-x}Al_x$, where x is 0, 0.4, 1, 3, 6, and 9, and on $Ce_2Fe_{14}Si_3$. For comparison with a nonmixed valency material, we have also studied the neodymium L_{III} edge in the $Nd_2Fe_{17-x}Al_x$ solid solutions, where $x=0$, 3, and 8. Further the iron K-edge spectra of all the compounds have been measured.

II. EXPERIMENT

The samples used for this study were prepared as described[9,10] earlier. The x-ray-absorption spectra have been measured with the synchrotron radiation provided by the DCI storage ring of the Laboratoire pour l'Utilisation du Rayonnement Electromagnétique, LURE, in Orsay, France. The compounds were measured at the D42 experimental station, which uses a channel cut silicon (331) crystal monochromator. The x-ray-absorption measurements were carried out in the transmission mode using ion chambers filled with helium-neon, both in front and behind the sample. The powder absorbers had a thickness of 9 to 13 mg/cm^2 at the cerium or neodymium L_{III} edges and of 3 to 4 mg/cm^2 at the iron K edge. The x-ray-absorption near-edge spectra, XANES, were recorded with a 0.25 eV step over an energy range starting at 120 eV below the edge.

During the processing of the XANES data, a linear background was subtracted from the experimental spectrum by extrapolating a least-squares fit of the pre-edge experimental data points. The maximum of the first derivative of a metallic foil spectrum, corresponding to the first inflection point in the absorption curve, was used as the metal K-edge or L_{III}-edge reference energy. For energy calibration, the spectrum of a thin metallic foil of chromium or iron, for the cerium and neodymium L_{III} edges or for the iron K edge, respectively, was recorded. Spectra were normalized by taking as unit absorbance the intersection point between the atomic background and the first EXAFS oscillation.

III. CERIUM L_{III}-EDGE XANES RESULTS AND ANALYSIS FOR $Ce_2Fe_{17-x}Al_x$ AND $Ce_2Fe_{14}Si_3$

The white lines observed at the L_{III} edge of rare-earth elements are usually assigned to transitions from the $2p_{3/2}$ to the $5d_{5/2}$ electronic states. For mixed valent rare-earth elements, such as cerium in transition metal intermetallic compounds, the study of the L_{III} edge permits the determination of the rare-earth $4f$ orbital occupation and, hence, its valence. Whereas in rare-earth elements, the $4f$ levels are strongly localized, in rare-earth transition metal intermetallic compounds, two different $4f$ configurations are possible,[12] the first with localized $4f$ electrons and the second with itinerant $4f$ electrons and a strong participation in the metallic bonding. In the second case, a core hole occurs in the ground state and is concommitantly followed by a relaxation of the $5d$ levels, which screens the core hole. Two possible transitions result at the L_{III} edge of the rare-earth element, transitions which have different energies and are assigned as transitions to the $5d_{5/2}$ level with screening of the core hole and to the $5d_{5/2}$ level without screening of the core hole, respectively. For cerium, these transitions are then associated with the $4f^1$ and $4f^0$ electronic configurations.

Figure 1 shows the XANES spectra of $Ce_2Fe_{17-x}Al_x$, where x is 0, 0.4, 1, 3, 6, and 9, at the cerium L_{III} edge. All these spectra show the characteristic two-peak structure associated with the cerium $4f^1$ and $4f^0$ configurations, at ca. 5728 and ca. 5736 eV, respectively, a structure which indicates that cerium is in a mixed valent state in these compounds. Further it is clear, even without any quantitative analysis, that the relative area of the $4f^1$ configuration is increasing with increasing x. This increase indicates that the cerium spectroscopic valence is decreasing with increasing x.

A quantitative determination of the cerium valence re-

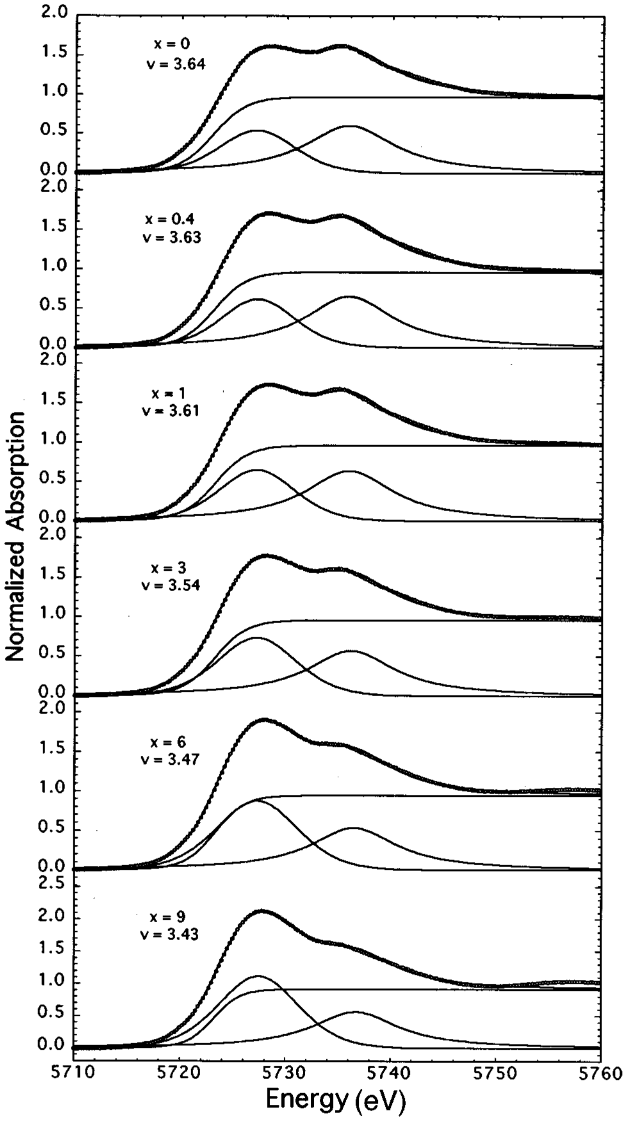

FIG. 1. Cerium L_{III}-edge XANES spectra of $Ce_2Fe_{17-x}Al_x$, where x is 0, 0.4, 1, 3, 6, and 9. The fits shown are model d described in the text.

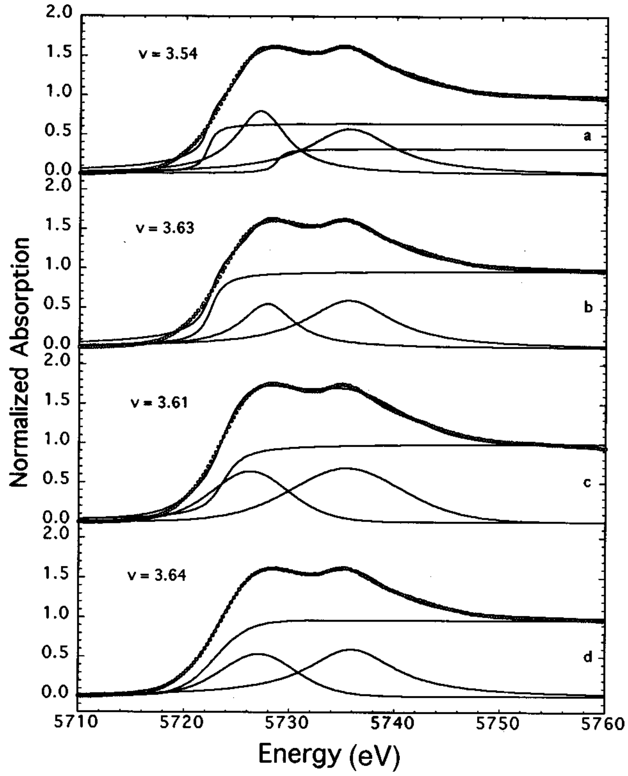

FIG. 2. Different model fits of the XANES spectrum of $Ce_2Fe_{16.8}$. See text for the description of the different fitting models a, b, c, and d.

quires a fit of the spectra in Fig. 1. In previous studies,[1–6] different fitting models have been used. All authors agree to fit[13] the continuous absorption from the $2p$ core hole with an arctanlike step function and to fit the peaks with Lorentzian functions. Capehart *et al.*[2,5] used one arctan function to fit the continuous absorption and two Gaussian-broadened Lorentzian functions. In contrast, Chaboy *et al.*[1] and Isnard *et al.*,[3,6] following Röhler's model,[13] used two arctan functions, one for each white line, and two Lorentzian functions. The spectroscopic cerium valence may be calculated from the relative weighted areas of the two Lorentzian functions.

In view of the different fitting models previously used in the literature, we have also tried different fitting models to analyze the XANES spectra of $Ce_2Fe_{17-x}Al_x$ shown in Fig. 1. Figure 2(a) shows, in agreement with Röhler's method,[13] the fit, which has a χ^2 of 0.338, of the XANES spectrum of $Ce_2Fe_{16.8}$ with two arctan and two Lorentzian functions. This model, denoted as a, can be modified by using only one arctan, model b, Fig. 2(b), with a χ^2 of 0.378, and, as reported by Capehart *et al.*,[2,5] by adding a Gaussian broadening of the Lorentzian functions, Fig. 2(c), for model c, with a χ^2 of 0.225. Figure 2(d) shows a fourth model, denoted d, with a χ^2 of 0.059, in which a sigmoidal function, rather than an arctan function is used to improve the pre-edge fit of the spectrum. In this case one Gaussian-broadened Lorentzian and one Lorentzian functions are used to fit the absorption peaks. The internally consistent values of the valence, deduced from fits with model d for the entire $Ce_2Fe_{17-x}Al_x$ series, and the excellent quality of these fits, lead us to prefer this model which will be used in all the following discussion. In addition, the use of a sigmoidal function instead of an arctan function can be rationalized as follows. The arctan function is the result of an infinite sum of Lorentzian functions, whereas the sigmoidal function is the result of an infinite sum of Gaussian broadened Lorentzian functions. We find, in agreement with Capehart *et al.*,[2,5] that the two peaks in the XANES spectra of the $Ce_2Fe_{17-x}Al_x$ solid solutions, see Fig. 1, are better fit with one Gaussian broadened Lorentzian and one Lorentzian functions. We believe that this broadening is due to the random occupation of the cerium near-neighbor sites by iron and aluminum.

Table I gives the cerium valence obtained with model d from the spectra shown in Fig. 1, as well as the corresponding cerium site volume. These volumes were computed from the crystallographic parameters given in Ref. 9 and by using the program described by Gelato.[14] In computing the site volume, cerium, and iron radii of 1.81 and 1.26 Å, respectively, were used and the planes of the Voronoi polyhedron were placed at a distance from the cerium atom which is proportional to these radii. No attempt was made to include

TABLE I. Cerium XANES absorption energies (ca. ±0.2 eV), valence, and site volume in $Ce_2Fe_{17-x}M_x$.

M	x	E_F, eV	E_{4f^1}, eV	E_{4f^0}, eV	ΔE, eV	Ce valence	V_{WS}, Å^3
Al	0	5722.9	4.2	13.0	8.8	3.64	30.65
	0.4	5722.8	4.5	13.2	8.7	3.63	30.80[a]
	1	5723.2	4.1	12.8	8.7	3.61	31.03
	3	5723.3	4.0	13.0	9.0	3.54	31.73
	6	5723.3	4.0	13.2	9.2	3.47	32.60
	9	5723.2	4.4	13.4	9.0	3.43	33.26
Si	3	5723.3	4.1	13.2	9.1	3.56	30.37

[a]Value interpolated between $x=0$ and 1.

the aluminum atoms in these calculations. This method differs from that used by Capehart *et al.*,[2] who only used the iron radius in computing the cerium site volume. We believe that the use of the 1.81 Å cerium radius does not bias our results and conclusion, because we are always comparing compounds within a given series. To make a direct comparison between the site volumes calculated herein and those calculated by Capehart *et al.*,[2] a scaling factor of 1.02 could be applied. Figure 3 shows that the cerium valence correlates linearly with the cerium site volume in $Ce_2Fe_{17-x}Al_x$, and also shows data from Ref. 2, data which have not been rescaled.

In conclusion, our measurements on $Ce_2Fe_{17-x}Al_x$ confirm and extend the steric effect observed by Capehart *et al.*[2,5] Further, the substitution of aluminum for iron influences the cerium valence, whose value decreases from 3.64 in Ce_2Fe_{17} to 3.43 in $Ce_2Fe_8Al_9$. This change in valence is substantially larger than those reported for hydrogenation[3] or nitrogenation[6] of Ce_2Fe_{17}, but once again the difference may be related to different fitting procedures. The slopes of the cerium valence as a function of the unit cell volume in the $Ce_2Fe_{17}H_x$ series,[3] and in the $Ce_2Fe_{17-x}Al_x$ series are -1.71×10^{-3} and -2.36×10^{-3} Å^{-3}, respectively.

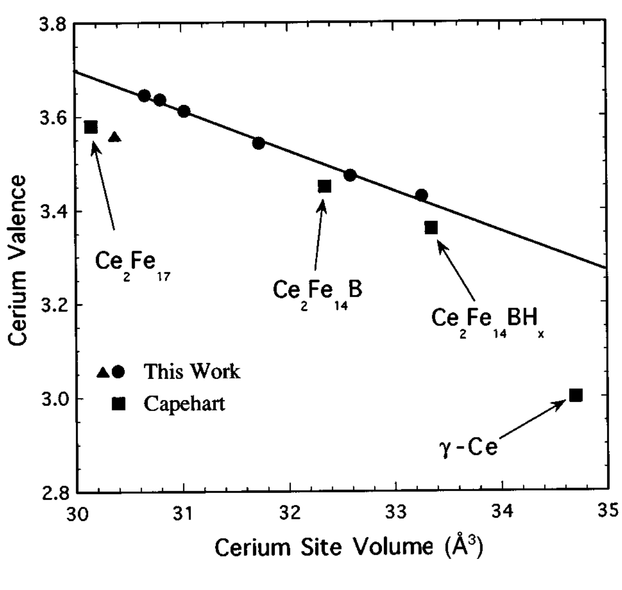

FIG. 3. The cerium spectroscopic valence versus the cerium site volume in $Ce_2Fe_{17-x}Al_x$, ●, $Ce_2Fe_{14}Si_3$, ▲, and in Ce_2Fe_{17}, $Ce_2Fe_{14}B$, $Ce_2Fe_{14}BH_x$, and γ cerium. The ■ data points were obtained from Ref. 2.

Hence, the cerium valence in $Ce_2Fe_{17-x}Al_x$ is more sensitive to a steric effect than is the $Ce_2Fe_{17}H_x$ series, perhaps because the additional hydrogen, which is a near neighbor of the cerium atom, forms additional bonds with the cerium atom. Finally, the difference of 0.06 in cerium valence reported for Ce_2Fe_{17} herein and in Ref. 2 should be addressed. We believe that this small difference is in large part due to a slightly different choice of the step function, because as is shown in Fig. 2, valence differences of 0.1 are obtained from different fitting models. However, the actual composition of our sample is $Ce_2Fe_{16.8}$ and the small iron deficiency may be responsible for the small difference in cerium valence.

The energy of the Fermi level, E_F, as determined from the energy of the maximum slope in the sigmoidal function, see Table I, is independent of aluminum content in the $Ce_2Fe_{17-x}Al_x$ solid solutions. The energies, relative to this Fermi level, of the two absorption peaks corresponding to the cerium $4f^1$ and $4f^0$ configurations, are also given in Table I. The energies of these peaks remain constant with increasing x within their experimental accuracy and, as expected,[15,16] the replicate splitting, ΔE, between these peaks is both relatively constant, with values between 8.7 and 9.1 eV, and independent of aluminum content. Virtually the same energies are obtained for $Ce_2Fe_{14}Si_3$.

The XANES spectrum at the cerium L_{III} edge of $Ce_2Fe_{14}Si_3$ was also analyzed with model *d* and a cerium valence of 3.56 was obtained. The cerium site volume, calculated as explained above, is 30.37 Å^3. As indicated by the triangle in Fig. 3, $Ce_2Fe_{14}Si_3$ does not follow the linear correlation observed for $Ce_2Fe_{17-x}Al_x$, in part because the unit cell volume of the $Ce_2Fe_{17-x}Si_x$ solid solutions uniquely decreases[10] as x increases. It is known from neutron diffraction measurements[10] that silicon substitutes preferentially on the 18*h* iron site in the Ce_2Fe_{17} structure, the site which has three, the largest number of cerium near neighbors. Electrical resistivity measurements[11] and Mössbauer spectral measurements[10] on the $Ce_2Fe_{17-x}Si_x$ solid solutions lead to the conclusion that silicon bonds covalently with its neighbors. This covalent bonding gives rise to a decrease in the cerium valence between $Ce_2Fe_{16.8}$ and $Ce_2Fe_{14}Si_3$, a decrease which more than compensates for the steric effect. As was shown previously,[6] the valence of cerium in $Ce_2Fe_{17}N_3$ is larger than would have been predicted from its unit cell volume, assuming the slope observed[3] for the $Ce_2Fe_{17}H_x$ series. However, this departure from the steric dependence of the cerium valence is opposite to that observed here for $Ce_2Fe_{14}Si_3$ and was attributed to bonding between the cerium and the interstitial nitrogen atoms.

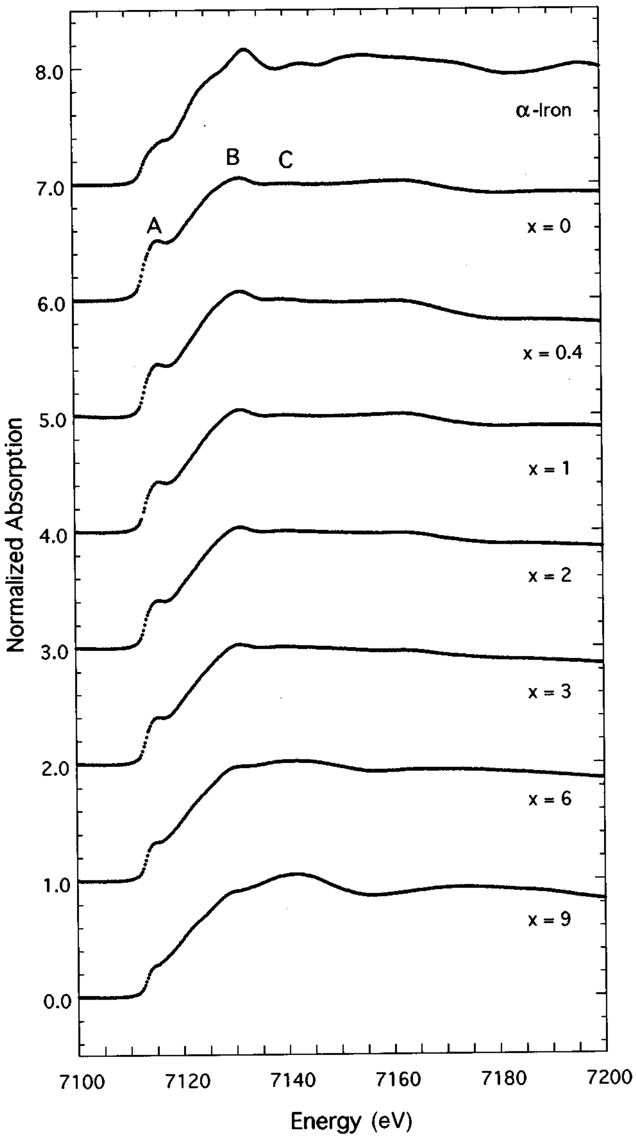

FIG. 4. Iron K-edge XANES spectra of $Ce_2Fe_{17-x}Al_x$, where x is 0, 0.4, 1, 3, 6, and 9. The spectrum of α iron is shown for comparison.

IV. IRON K-EDGE XANES RESULTS FOR $Ce_2Fe_{17-x}Al_x$ AND $Ce_2Fe_{17-x}Si_x$

Figure 4 shows the XANES spectra of the $Ce_2Fe_{17-x}Al_x$ solid solutions measured at the iron K edge. All of these spectra show a structure which is rather similar to that of α iron. There are three resolved peaks labeled A, B, and C, in Fig. 4. Their energies, $E_{A,B,C}$, as well as those for the $Ce_2Fe_{17-x}Si_x$ solid solutions, obtained from the first derivative of the spectra, are given in Table II, which, for comparison, also gives the energies of the corresponding peaks in α iron as well as the shift of the A, B, and C peaks, $\Delta E_{A,B,C}$, relative to the Fermi energy, E_F. The Fermi energy has been taken as the point of maximum slope in the absorption edge. Of course, the values given in Table II for the Fermi energy are measured from the iron $1s$ electronic shell and hence, differ in absolute value from the values given for the Fermi energy in Table I, values which are measured from the cerium $2p$ electronic shell. As indicated by the values given in Table II, there is no significant change of the Fermi energy in the $Ce_2Fe_{17-x}Al_x$ solid solutions with x. This is somewhat surprising because, as x increases the number of electrons in the unit cell decreases, and thus a decrease in the Fermi energy might be expected.

A visual inspection of the spectra shown in Fig. 4 indicates that there are changes in peaks, A, B, and C, with x. However, as indicated by the values given in Table II, there are at most small changes in their energies, $E_{A,B,C}$, and, hence, the apparent changes in the spectral shape are mainly due to changes in the relative intensities of the peaks.

Peak A in α iron is usually assigned[15] to a $1s \rightarrow 3d$ transition, a magnetic dipole forbidden transition which has a nonzero probability and intensity because of $4p$-$3d$ band mixing. Similarly, peak A in the $Ce_2Fe_{17-x}Al_x$ solid solutions is assigned to a $1s \rightarrow 3d$ transition. The energy of peak A, E_A, in the $Ce_2Fe_{17-x}Al_x$ solid solutions decreases slightly as x increases, such that ΔE_A is 2.9 and 1.7 eV above the

TABLE II. Energies (ca. ± 0.2 eV) in eV of the XANES transitions at the iron K edge.

Compound	x	E_F	E_A	ΔE_A	E_B	ΔE_B	E_C	ΔE_C
$Ce_2Fe_{17-x}Al_x$	0	7113.1	7116.0	2.9	7131.7	18.6	7140.5	27.4
	0.4	7113.3	7116.2	2.9	7131.5	18.2	7139.5	26.2
	1	7113.1	7116.2	3.1	7131.5	18.2	7140.2	27.1
	2	7113.1	7115.8	2.7	7131.5	18.4	7139.8	26.7
	3	7113.3	7115.7	2.4	7131.0	17.7	7139.0	25.7
	6	7113.3	7115.6	2.3	7131.6	18.3	7142.0	28.7
	9	7113.3	7115.0	1.7	7130.4	17.1	7141.5	28.2
$Ce_2Fe_{17-x}Si_x$	0.2	7113.3	7116.3	3.0	7131.9	18.6	7139.9	26.6
	2	7113.1	7116.1	3.0	7131.2	18.1	7139.5	26.4
	3	7113.1	7116.1	3.0	7130.9	17.8	7140.0	26.9
$Nd_2Fe_{17-x}Al_x$	0	7113.1	7115.8	2.7	7131.4	18.3	7141.7	28.6
	3	7113.3	7115.6	2.3	7130.9	17.6	7141.2	27.9
	8	7113.1	7114.8	1.7	7130.4	17.3	7141.7	28.6
α-Fe		7113.3	7117.8	4.5	7131.8	18.5	7143.3	30.0

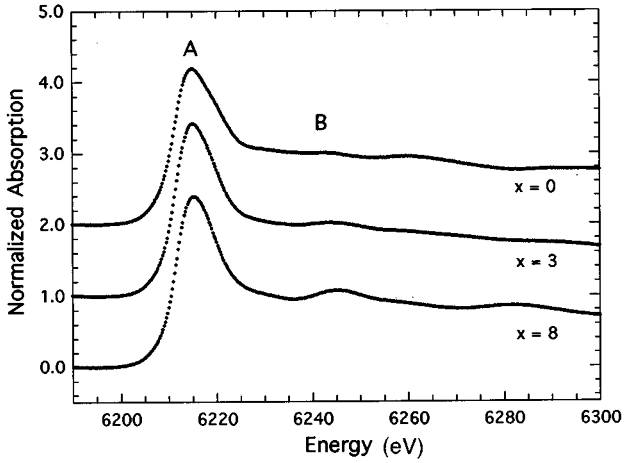

FIG. 5. Neodymium L_{III}-edge XANES spectra of $Nd_2Fe_{17-x}Al_x$, where x is 0, 3, and 8.

Fermi energy, for $x=0$ and 9, respectively. As will be dis2cussed below, the $Nd_2Fe_{17-x}Al_x$ solid solutions show a very similar decrease in E_A and ΔE_A as x increases from 0 to 8. In contrast, the $Ce_2Fe_{17-x}Si_x$ solid solutions show no variation of E_A and ΔE_A with x, at least over the limited solubility range of $x=0$ to 3.

First principle calculations[17] of the electronic structure of the $Nd_2Fe_{17-x}Al_x$ solid solutions, for $x=0$, 1, 2, and 4, give the density of iron $3d$ states from 10 eV below to 10 eV above the Fermi energy and indicate that there are unoccupied $3d$ states in the region up to ca. 4 eV above the Fermi energy. This agrees with the assignment of peak A in the spectra shown in Fig. 4. The intensity of peak A clearly decreases with increasing x, in agreement with the smaller number of unoccupied iron $3d$ states expected as the aluminum content increases in the $Ce_2Fe_{17-x}Al_x$ solid solutions.

Peaks B and C in α iron are due[15] to multiple scattering by the first three shells of iron near neighbors. Thus, we assign peaks B and C to multiple scattering by the first three shells of iron near neighbors in the $Ce_2Fe_{17-x}Al_x$ solid solutions and, in agreement with the cell expansion,[9] the peaks show a small but nonuniform decrease in energy relative to the Fermi energy with increasing x. In these solid solutions, the four crystallographically distinct iron sites have[18] first neighbor shells at distances between 2.5 and 3.3 Å, second neighbor shells at distances between 4.2 and 4.5 Å, and third neighbor shells at distances between 5.2 and 5.8 Å. These shells all contain three kinds of atoms, iron, aluminum, and cerium. Hence, multiple scattering calculations for these solid solutions would be very difficult. We believe that the changes in the relative intensities of peaks B and C are related to changes in the nature of the atoms in the different shells, particularly to the replacement of iron by aluminum, a replacement which enhances peak C.

V. NEODYMIUM L_{III}-EDGE AND IRON K-EDGE XANES RESULTS FOR $Nd_2Fe_{17-x}Al_x$

In order to compare the results obtained on the $Ce_2Fe_{17-x}Al_x$ and $Ce_2Fe_{17-x}Si_x$ solid solutions, in which cerium is mixed valent, with nonmixed valence compounds, we have also carried out neodymium L_{III}-edge and iron K-edge XANES measurements on the $Nd_2Fe_{17-x}Al_x$ solid solutions, solid solutions in which neodymium is always expected to be trivalent. Figure 5 shows the neodymium L_{III}-edge XANES measurements on the $Nd_2Fe_{17-x}Al_x$ solid solutions, for x equal to 0, 3, and 8. The energy of the Fermi level and the energies of the observed peaks, relative to the Fermi energy, are given in Table III. The single peak at ca. 6215 eV, whose energy, ΔE_A, is virtually independent of x, indicates that neodymium is indeed trivalent in these solid solutions. The absorption area between 6190 and 6230 eV under the curves for $x=8$ in Fig. 5 is larger than the area under the curve for $x=0$. This increase in absorption area, when aluminum is substituted to iron, indicates an increase in the empty $5d$ state density and hence, a decrease in the $5d$-$3d$ hybridization.

TABLE III. Neodymium XANES absorption energies (ca. ± 0.2 eV) in $Nd_2Fe_{17-x}Al_x$.

x	E_F, eV	ΔE_A, eV	ΔE_B, eV
0	6212.1	2.8	31.0
3	6212.4	2.8	31.5
8	6212.1	3.1	32.6

Figure 6 shows the iron K-edge XANES measurements on the $Nd_2Fe_{17-x}Al_x$ solid solutions, for x equal to 0, 3, and 8. The Fermi energies, E_F, and the energies, $E_{A,B,C}$, and their shifts relative to the Fermi energy, $\Delta E_{A,B,C}$, of peaks A, B, and C, have been measured as explained above and are given in Table II. The changes observed as x increases from zero to eight are similar to those described above for the $Ce_2Fe_{17-x}Al_x$ solid solutions. Hence peak A is assigned to a $1s \rightarrow 3d$ transition in agreement with the electronic structure[17] of the $Nd_2Fe_{17-x}Al_x$ solid solutions for $x=0$, 1, 2, and 4, a structure which shows that there are unoccupied $3d$

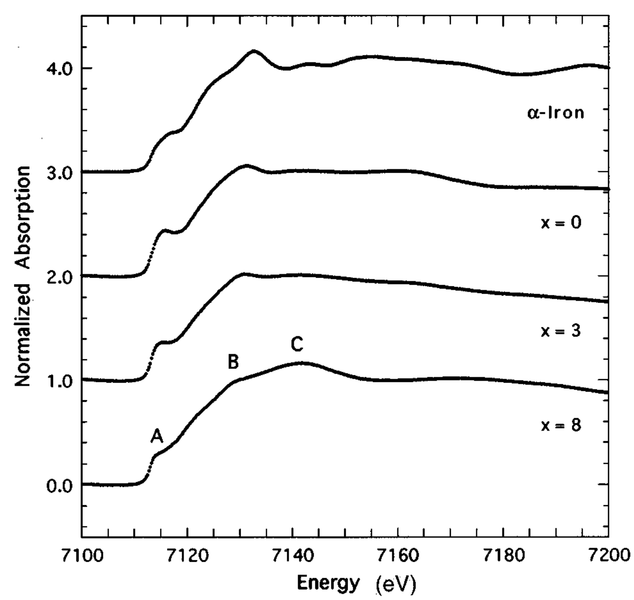

FIG. 6. Iron K-edge XANES spectra of $Nd_2Fe_{17-x}Al_x$, where x is 0, 3, and 8. The spectrum of α iron is shown for comparison.

states in the region up to ca. 4 eV above the Fermi energy. Furthermore, the increase in the intensity of peak *C* in both the $Ce_2Fe_{17-x}Al_x$ and $Nd_2Fe_{17-x}Al_x$ solid solutions, as x increases from zero to nine and zero to eight, respectively, supports the above conclusion that the relative intensities of peaks *B* and *C* are determined by the number and distance of the iron neighbors in the subsequent shells of neighbors. Indeed, neutron diffraction measurements[9,18] have shown that the aluminum substitutional pattern is identical in both sets of solid solutions. More specifically, aluminum prefers the 18*h* site for x smaller than 6, and the 6*c* site for x greater than 6. It is worth noting that peak *C* dominates over peak *B* for x between six and nine in Fig. 4 and for x equal to eight in Fig. 6. We tentatively conclude that the predominance of peak *C* results from the preferential occupation of the 6*c* site by aluminum.

VI. CONCLUSIONS

The cerium L_{III}-edge XANES study of the $Ce_2Fe_{17-x}Al_x$ solid solutions shows that the cerium is mixed valent and its valence decreases linearly with increasing cerium site volume and increasing x and hence, confirms the steric effect observed by Capehart *et al.*[2] in their study of $Ce_2Fe_{14}B$ and related compounds. A comparison of the slopes of the cerium valence with increasing unit cell volume in the $Ce_2Fe_{17-x}Al_x$ series and in the $Ce_2Fe_{17}H_x$ series[3] indicates that both a steric and a bonding effect on the cerium valence are present in the second series. A similar near-neighbor bonding effect is observed in $Ce_2Fe_{14}Si_3$ and supports the covalent bonding between cerium and silicon already observed by Mössbauer spectroscopy and electrical resistivity measurements.[10,11] In contrast, the neodymium L_{III}-edge XANES study of the $Nd_2Fe_{17-x}Al_x$ solid solutions indicates that neodymium is trivalent. Further, the increase in absorption area with increasing x indicates a decrease in the $5d$-$3d$ hybridization.

The iron K-edge XANES spectra of the $Ce_2Fe_{17-x}Al_x$ and $Nd_2Fe_{17-x}Al_x$ solid solutions show three main peaks. Peak A at ca. 2.5 eV above the Fermi level is assigned to a $1s \rightarrow 3d$ transition in agreement with band structure calculations.[17] Peaks *B* and *C* are assigned to multiple scattering by the first three shells of near-neighbor atoms and their energy and intensity reflect the complex changes in the near-neighbor environment and the unit cell expansion occurring when aluminum is substituted in place of iron.

ACKNOWLEDGMENTS

The authors acknowledge, with thanks, the Division of Materials Research of the U.S. National Science Foundation, for Grants No. DMR-92-14271 and No. 95-21739, the Ministère de la Communauté Française of Belgium for Grant No. A.R.C. 94/99-175, and the Stichting voor Fundamenteel Onderzoek der Materie, which is financially supported by the Nederlandse Organisatie voor Wetenschappelijk Onderzoek.

[1] J. Chaboy, J. Garcia, A. Marcelli, O. Isnard, S. Miraglia, and D. Fruchart, J. Magn. Magn. Mater. **104-107**, 1171 (1992).

[2] T. W. Capehart, R. K. Mishra, G. P. Meisner, C. D. Fuerst, and J. F. Herbst, Appl. Phys. Lett. **63**, 3642 (1993).

[3] O. Isnard, S. Miraglia, D. Fruchart, C. Giorgetti, S. Pizzini, E. Dartyge, G. Krill, and J. P. Kappler, Phys. Rev. B **49**, 15 692 (1994).

[4] J. Chaboy, J. Garcia, and A. Marcelli, Appl. Phys. Lett. **65**, 3149 (1994).

[5] T. W. Capehart, R. K. Mishra, G. P. Meisner, C. D. Fuerst, and J. F. Herbst, Appl. Phys. Lett. **65**, 3151 (1994).

[6] O. Isnard, S. Miraglia, D. Fruchart, C. Giorgetti, E. Dartyge, and G. Krill, J. Phys. Condens. Matter **8**, 2437 (1996).

[7] D. Fruchart, F. Vaillant, A. Yaouanc, J. M. D. Coey, R. Fruchart, Ph. L'Héritier, T. Riesterer, J. Osterwalder, and L. Schlapbach, J. Less-Common Met. **130**, 97 (1987).

[8] D. P. Middleton and K. H. J. Buschow, J. Alloys Compd. **203**, 2117 (1994).

[9] S. R. Mishra, G. J. Long, O. A. Pringle, D. P. Middleton, Z. Hu, W. B. Yelon, F. Grandjean, and K. H. J. Buschow, J. Appl. Phys. **79**, 3145 (1996).

[10] D. P. Middleton, S. R. Mishra, G. J. Long, O. A. Pringle, Z. Hu, W. B. Yelon, F. Grandjean, and K. H. J. Buschow, J. Appl. Phys. **78**, 5568 (1995).

[11] D. Vandormael, F. Grandjean, H. Bougrine, M. Ausloos, D. P. Middleton, K. H. J. Buschow, and G. J. Long, J. Appl. Phys. **81**, 2643 (1997).

[12] M. S. S. Brooks and B. Johansson, in *Handbook of Magnetic Materials*, edited by K. H. J. Buschow (North-Holland, Amsterdam, 1993), Vol. 7, Chap. 3.

[13] J. Röhler, in *Handbook on the Physics and Chemistry of Rare Earths*, edited by K. A. Gschneidner, J. R. Eyring, and S. Hufner (Elsevier, New York, 1987), Vol. 10, Chap. 71.

[14] L. Gelato, J. Appl. Crystallogr. **14**, 141 (1981).

[15] A. Bianconi, in *X-ray Absorption: Principles, Applications, Techniques of EXAFS, SEXAFS, and XANES*, edited by D. C. Koningsberger and R. Prins (Wiley, New York, 1988), Chap. 11.

[16] J. F. Herbst and J. W. Wilkins, Phys. Rev. B **26**, 1689 (1982).

[17] M. Z. Huang and W. Y. Ching, J. Appl. Phys. **76**, 7046 (1994).

[18] G. J. Long, G. K. Marasinghe, S. Mishra, O. A. Pringle, Z. Hu, W. B. Yelon, D. P. Middleton, K. H. J. Buschow, and F. Grandjean, J. Appl. Phys. **76**, 5383 (1994).